Avionics System for Aggressive Maneuvers

V. Gavrilets, A. Shterenberg, I. Martinos, K. Sprague, M.A. Dahleh & E. Feron
M.I.T.

ABSTRACT

An Xcell-60 5 foot rotor diameter hobby helicopter was instrumented to perform autonomous aggressive maneuvers. The avionics system, state estimator design, and vibration isolation are presented. An analysis of helicopter dynamics based on manual flight data is given.

INTRODUCTION

Recently there has been considerable interest in the applications of small, unmanned helicopters. Most of the research has been concentrated on achieving greater autonomy; for example, using imaging sensors to perform navigation tasks [6]. One interesting feature of such helicopters is their outstanding maneuverability [5], because they are not constrained by a human presence onboard. A small hobby helicopter with a vibration mounted film camera was used to create a highly agile falcon-eye video for a National Geographic TV documentary, aired January 9, 2000 on CNBC. During the videotake, a 5 foot rotor diameter helicopter was manually flown between skyscrapers in the Bronx. The wide maneuver envelope and hovering capability of small helicopters can also potentially be used in urban warfare.

To make aggressive maneuvering safer and decrease overarching dependence on the skills of a pilot, it is necessary to design a feedback control system with an adequate closed loop bandwidth. Vibration isolation with proper frequency characteristics is essential for the high-g flight of a rotorcraft. We are preparing a demonstration of a fully autonomous flight featuring aggressive maneuvers, including the split-S and longitudinal loop. This paper describes an avionics system we implemented to achieve high-bandwidth feedback control with robustness to modeling errors, gusts, and vibrations.

Author's Current Address:
V. Gavrilets, A. Shterenberg, I. Martinos, K. Sprague, M.A. Dahleh and E. Feron, M.I.T., Cambridge, MA 02139, USA.

Based on a presentation at DASC 2000.

0885/8985/01/$10.00 © 2001 IEEE

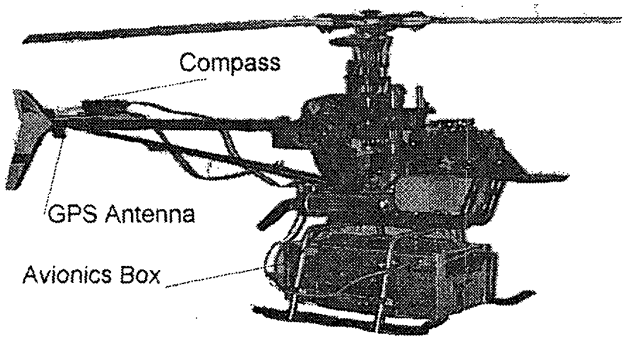

Fig. 1. M.I.T. Xcell-60 with avionics system

DESCRIPTION OF A TEST VEHICLE

Our test vehicle, shown in Figure 1, is an alcohol-powered Xcell-60 hobby helicopter.

It has a two-blade rotor augmented with a Bell-Hiller stabilizing bar. The rotor has a diameter of 5 foot with a speed range of 1500-1700 RPM. The gross takeoff weight (with 7 pounds of avionics added to the airframe) is 18 pounds. A well-trained RC pilot has performed high-speed 2 g turns, full longitudinal loops, high-rate stall turns and snap-rolls with the data-acquisition payload. A subset of recorded state trajectories and pilot commands during a snap roll maneuver are given in Figure 3. An electronic governor maintains the commanded rotor speed with a maximum observed tracking error of 40 RPM by adjusting throttle commands. A hobby gyro provides proportional negative feedback of measured yaw rate to tail rotor pitch, thereby augmenting yaw rate damping. Three other actuators control the lateral and longitudinal cyclic pitch, and the collective pitch of the main rotor blades.

The helicopter was equipped with a data acquisition system. All vibration sensitive equipment is contained in the avionics box (Figure 2) mounted on elastomeric isolators, which were chosen and located in such a way that the rotational and

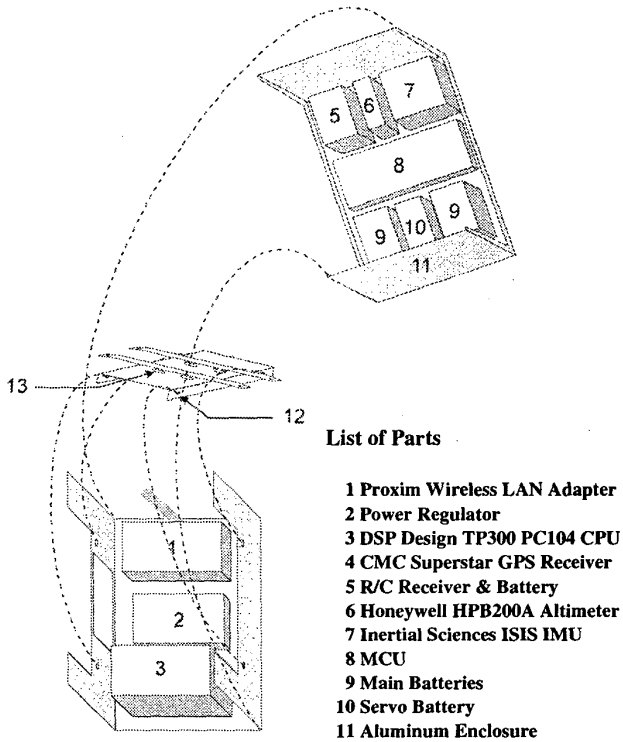

List of Parts

1 Proxim Wireless LAN Adapter
2 Power Regulator
3 DSP Design TP300 PC104 CPU
4 CMC Superstar GPS Receiver
5 R/C Receiver & Battery
6 Honeywell HPB200A Altimeter
7 Inertial Sciences ISIS IMU
8 MCU
9 Main Batteries
10 Servo Battery
11 Aluminum Enclosure
12 Mounting Bracket
13 ME500-1 Neoprene Isolators

Fig. 2. Vibration-isolated avionics assembly

translational vibration inputs are well attenuated. Vibration issues are described later in detail.

HELICOPTER DYNAMICS AND STATE ESTIMATION

The flight sensors were chosen such that all relevant state vector elements can be estimated with a reasonable bandwidth (10-15 rad/sec depending on the state). Some full state feedback design methods, like linear quadratic regulators, are well known to provide excellent robustness to modeling errors, with a 60° phase margin and one-half to infinity gain margin in any actuator path. This is essential, since it is rather difficult to model or identify rotorcraft dynamics accurately, especially in fast forward flight. Full state feedback also suppresses undesirable cross-axis responses much better than independent single-input-single-output feedback loops, given similar closed loop bandwidth. In addition, availability of a full state estimate makes the system identification problem significantly easier. Thus, our goal is to select the set of states such that the dynamics (including cross-axis responses!) are adequately represented up to a certain bandwidth. The rest of the dynamics, like servo responses, can then be modeled by transfer functions. These additional lags must be taken into account when selecting the closed loop bandwidth of the system.

Linearized rigid-body dynamics for most helicopters can be adequately described by 8 states, namely 3 body axis velocities, 3 inertial angular rates, and Euler roll and pitch attitude angles [1]. The heading angle and geographical location are irrelevant for aircraft stability analysis, but are needed for outer guidance loops. Occasionally, the state vector is augmented with two states corresponding to the Bell-Hiller stabilizer bar dynamics. The stabilizer bar improves damping of unstable lateral and longitudinal phugoid modes at the expense of a lagged response to cyclic inputs. The authors of [2] estimated that a stabilizer bar on a much larger Yamaha R-50 helicopter contributes a lag with a time constant of roughly 5 rotor revolutions to lateral and longitudinal pitch cyclic actuation. The rotor speed at hover on the R-50 is 850 RPM [2], which resulted in the estimated time constant of 0.38 seconds, or roughly a 2.5 rad/sec cutoff frequency. This is rather close to the rigid body modes of the helicopter, and as a result a model that couples flybar and angular rate states was used in [2] for system identification. The Xcell-60 rotor speed is roughly two times higher, which leads to the estimated lag of approximately 0.2 seconds. This estimate is well supported by flight data: we applied a first order filter with a time constant of 0.2 seconds and a gain of 20 (deg/sec)/degree to the longitudinal cyclic pitch. A filter with the same time constant and a gain of 30 (deg/sec)/degree was applied to the lateral cyclic pitch. The higher gain in the roll channel is due to lower roll inertia. The results are compared with pitch and roll rate time histories in Figure 4. During this segment, the pilot

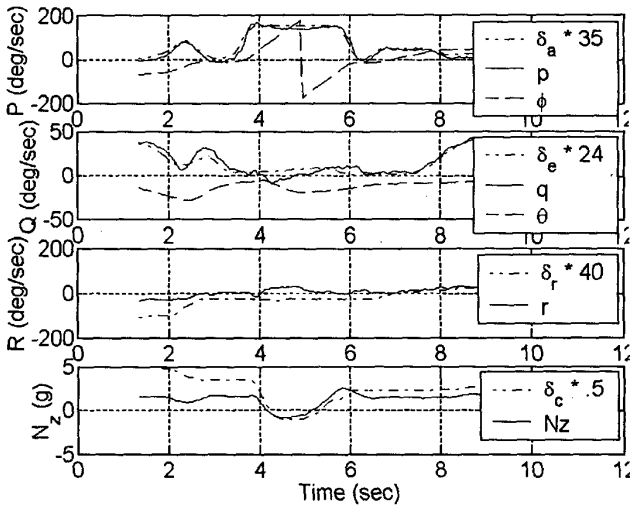

Fig. 3. State and control trajectories during snap roll maneuver

performed a 2-g turn at a forward speed of 10 m/seconds. Time histories of roll and pitch Euler angles are included for completeness.

We feel that it is adequate for flight control design purposes to model the effect of the flybar by two first order lags, neglecting coupling between flybar states and pitch and roll angular rates. In fact, because of the relatively stiff rotor blades, R/C pilots perceive cyclic inputs on such helicopters as a slightly lagged rate control system, which is well illustrated in Figure 4. This actuation lag requires that the crossover frequency in a rate-tracking loop not be pushed beyond roughly 5 rad/sec in order to retain adequate phase margin. The advantage of this modeling approach is that the flybar states do not have to be measured for feedback. Note that human pilots can perform exceptionally agile maneuvers without knowing the flybar position.

The yaw rate gyro is set to provide proportional feedback to tail rotor pitch, therefore, it does not require additional states for modeling. For modeling purposes the feedback gain setting of a gyro can be easily measured by swinging it from suspension and measuring the angular deflection of the servo. The maximum servo deflection is proportional to the maximum angular rate, which is a product of the maximum angular deflection of a swinging pendulum and its natural frequency.

In addition to the aforementioned eight states, we would like to estimate the heading and 3D inertial position vector for a fully autonomous flight. An inertial measurement unit, consisting of three gyros and three accelerometers, provides high-bandwidth information about the state vector. The main source of error in the integration of rotational and translational inertial navigation equations is the drift of the gyros. Therefore, we implemented a 13-state extended Kalman filter (EKF). The EKF state vector includes three inertial positions, three inertial velocities resolved in the body axis, four elements of a quaternion representation of attitude, and three rate gyro biases. Note that the gyro biases drift over time and this drift turns out to be significant for our duration of flight (15 minutes). It is highly beneficial to include gyro biases as states, since then an attitude estimate can be derived by dead-reckoning during short GPS outages. On the other hand, accelerometer biases are relatively small (within 10 mg), and they introduce small errors to the attitude estimate. The state vector is propagated at 25 Hz with a 4^{th} order Runge-Kutta algorithm (the IMU is sampled at 100 Hz). Once-per-second measurement updates are available from the GPS unit (3D inertial position and velocity), barometric altimeter, and magnetic compass. The roll and pitch rate gyro biases are well observable in the horizontal GPS position and velocity measurements. Yaw rate bias can be compensated for by the compass magnetic heading measurement. Heading errors also become observable in horizontal GPS velocity measurements during lateral maneuvers. The GPS vertical velocity and pressure altitude measurements are used to compensate for vertical accelerometer bias. Note that this state estimator design is quite robust to short GPS outages. After convergence of gyro bias estimate errors to 0.01 deg/sec, the helicopter

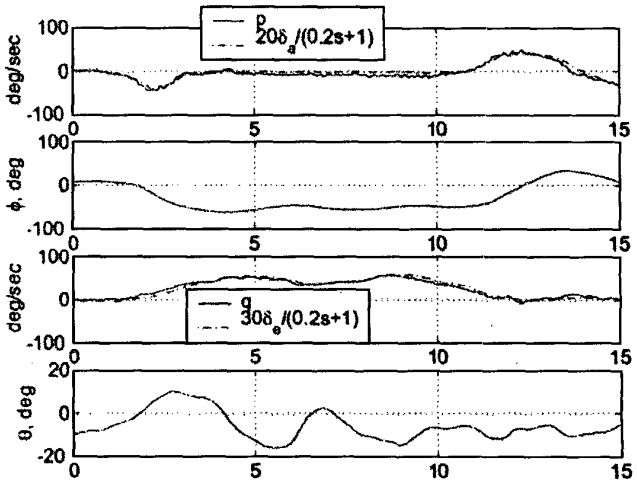

Fig. 4. Angular rate response to cyclic commands

attitude can be estimated to within 1 degree for around 1 minute, which provides plenty of time for the safety pilot to switch to manual control. In addition, the barometric altimeter will keep up-to-date altitude reference.

Note that the velocities are measured w.r.t. inertial frame, and not w.r.t. air. Therefore, steady winds and gusts have to be treated as disturbances by the control system. Since our goal is to demonstrate fully autonomous aggressive maneuvers, we impose a limit of 10-knot winds for flight operations.

The next section provides a more detailed description of the flight sensors, as well as the computers and servos used in the avionics system.

AVIONICS DESCRIPTION

Safety, the high bandwidth requirement for the flight control system, and adequate sensor information were key factors in designing the avionics package. The appendix contains the block diagram of the electronic components and their interconnections.

Computing and Telemetry

Most of the processing is done in the Central Processing Unit (CPU). The CPU is a 266 MHz PC104 board with 32 MB of RAM and 16 MB of permanent flash RAM (TP300 model by DSP Design). The input and output channels of the CPU include 4 serial ports, 4 A/D channels, and ethernet and parallel ports, most of which are used by the sensors and actuators. The CPU runs the real-time operating system QNX.

In order to allow for helicopter recovery in the case of CPU or main battery failure, a separate micro controller board, labeled MCU, handles the task of driving the servo actuators. Five servos are required to fly the helicopter; thus, the MCU has five output channels. The MCU was designed to allow the helicopter to be flown by either the CPU or an R/C pilot. These modes can be selected with the flip of a switch on the R/C

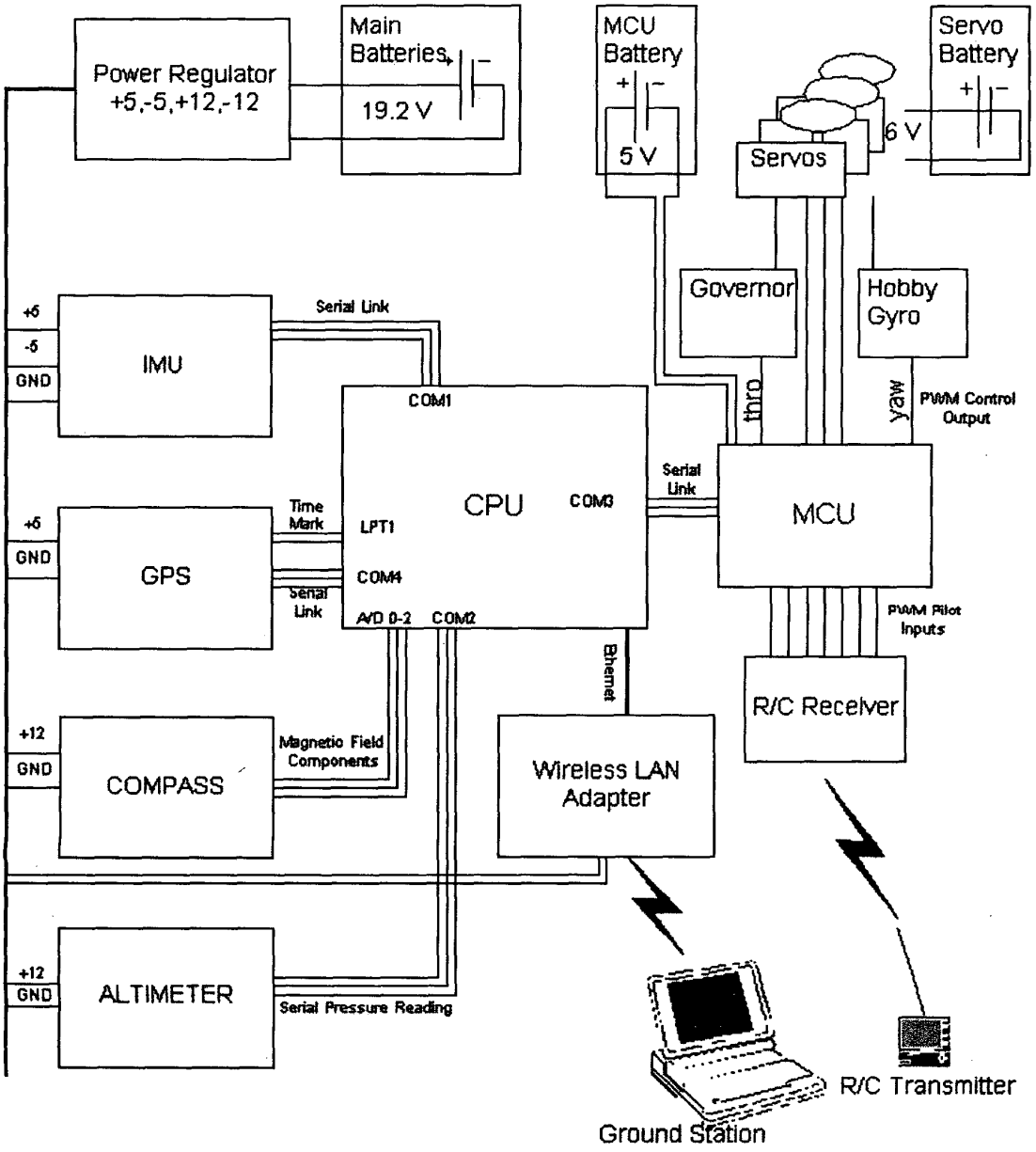

Fig. 5. Avionics diagram

transmitter. The MCU communicates with the CPU through a bi-directional serial interface; with the pilot through seven input channels. The input channels are used to measure pulses generated by the R/C receiver directly controlled by the pilot.

The MCU was implemented using two SX28 micro controllers and one PIC16F877. Multiple micro-controllers were used in order to achieve accurate pilot command measurements while generating output pulses in parallel. The board is powered separately from the CPU for safety reasons. Other features of the board include input filtering, optically isolated outputs, and a battery monitoring circuit.

The CPU communicates with the ground station via a wireless LAN telemetry system. While wireless LAN offers the benefit of high throughput, its poor reliability and timing prompted the decision to leave the telemetry system out of safety critical loops. The wireless LAN link is used only for monitoring and data logging. Having an ethernet link also proved to be an extremely valuable debugging tool. The Proxim RangeLAN2 ethernet adapter was chosen for the task. The adapter offers a bandwidth as high as 1.6 Mbits/s for large packets. Since it connects to an existing ethernet controller, Proxim did not require writing any QNX drivers.

The CPU and MCU hardware and software are completely duplicated in the hardware-in-the-loop simulator, while previously recorded sensor data is replayed through the serial port of a desktop computer. Models and flight software are thereby tested in a safe, low-risk environment.

Sensors

The Inertial Measurement Unit (IMU) provides the bulk of the sensor information to the CPU. The unit contains three gyroscopes and three accelerometers. The outputs of the sensors are temperature compensated internally. The IMU, manufactured by Inertial Sciences Inc., was chosen for its accuracy over an extended input range and for its light weight of only 250 grams. After a 10-minute preflight warm-up, the biases of the gyros drift on average by .03 degrees/second and the biases of the accelerometers drift by 5 mg during a 15-minute flight. The full scale of the gyros was chosen at ±300 deg/sec to enable high-rate maneuvers around any axis. The IMU provides 100 Hz updates of the rates and specific forces through the 115.2 Kbit/second serial port.

The Superstar GPS receiver from Canadian Marconi provides 1 Hz updates of the inertial position and velocity. Since the practice of scrambling GPS signals for civilian users, known as Selective Availability, was discontinued on May 1, 2000, short-term relative navigation with GPS provides horizontal accuracy on the order of several meters. The main source of GPS errors, in the absence of selective availability is ionospheric delay, and since the path traveled by a signal from a satellite to the helicopter does not change significantly in the fuel-limited flight duration of 15 minutes, the errors are small. Blending GPS and IMU measurements, as well as other sensory data in the EKF further improves navigation accuracy. Therefore, it is unnecessary to use differential GPS for a fully autonomous 15-minute flight.

The triaxial magnetoresistive sensor HMC2003, from Honeywell, was initially used to measure three components of the Earth's magnetic field in projection to the body axis. It was mounted on the tailboom, far away from the engine and avionics box. Experiments have shown that the compass requires cumbersome pre-flight 3D scale factor and bias calibration to compensate for magnetic fields induced by helicopter-mounted components. Since heading errors on the order of 15 degrees are tolerable for our application, the magnetometer was eliminated.

The HPB200A barometric altimeter, from Honeywell, is used to provide additional altitude information to GPS measurement. This is an absolute pressure sensor with the range 0-17 psi. The sensor resolution is 0.001 psi, which is roughly 2 feet, and the reading is quite stable. The altimeter is sampled 5 times per second. The pressure change due to induced velocity from the rotor turns out to be small. According to the momentum theory, dynamic pressure change due to induced velocity at hover is equal to T/4/A [3], where T is thrust, and A is rotor disc area. For our helicopter with 18 pounds gross weight and 5 foot rotor diameter this value is 0.0016 psi, which results in roughly 3 feet of altitude error. A wind of 10 knots induces the same error. Effects of gusts and thrust variations due to collective changes are of the same order, and these higher-frequency errors are low-pass filtered by a mechanical low-pass filter (a ping-pong ball with two small orifices) and the EKF.

Actuators

High bandwidth servos, especially for the tail rotor pitch, are essential to achieve a closed loop bandwidth adequate for aggressive maneuvers, without compromising stability. Fast hobby servos were chosen for all channels except throttle, where the response is dominated by the slow time constant of the engine. JRDS8417 servos were used. Their slew rate is 600 degrees/second, which translates to roughly a 7 Hz bandwidth (frequency at which 90 degrees phase lag occurs). Experiments with similar hobby servos (Futaba 9402, JR2700G), conducted by one of the authors, showed that they retain bandwidth when loaded to less than half the maximum rated torque. The servos are included as a part of our hardware-in-the-loop simulation to ensure that lag and quantization effects on closed loop operation are captured.

VIBRATION ISOLATION AND PREFILTERING

The vibration environment of a small helicopter is complex. The main source of large-amplitude high-frequency vibration inputs is the main rotor, spinning at roughly 26-27 Hz. The harmonics are 1 per revolution, 2 per revolution (blade passage frequency near tail rotor), the engine frequency (around 160 Hz), and the tail rotor frequency (around 115 Hz). These inputs also have sidebands, which excite lateral and vertical first bending modes of the tailboom (20 Hz). These inputs combined have amplitudes on the order of 40 deg/sec and 1 g in all axes, and have to be attenuated to make use of gyro and accelerometer data. Passive vibration isolation was designed for the avionics box weighing 7 pounds. The resulting rotational cutoff frequencies are in the range of 7-9 Hz, and translational frequencies of 11 Hz in horizontal plane, and 13 Hz in vertical direction. The cutoff frequencies must be low enough to provide sufficient attenuation of high-frequency vibration sources, while, at the same time, the suspension system should be sufficiently stiff to sustain high-g maneuvers without bottoming out. Low rotational cutoff frequencies were achieved by closely spacing the isolators inside the avionics box (Figure 2). The isolators were located in the corners of a rectangle, the geometric center of which coincides with the center of gravity of the isolated assembly. This construction serves to decouple rotational and translational modes [4]. Neoprene isolators (ME500-1 from Barry Controls) were chosen for their availability and low cost ($10 apiece). Neoprene has a damping ratio of 0.05, which results in the fast decay of transmissibility function, but also has 10:1 amplification factor at resonance. The suspended assembly resonances are excited by broadband vibration inputs. Since these resonant frequencies are significantly faster than helicopter rigid-body dynamics, we used digital notch filters to remove these modes. A higher damping material, like Barry-LT compound, would be beneficial.

The suspension assembly attenuates high-frequency vibration inputs to negligible levels. However, due to the main rotor hub arrangement, the helicopter has two low-frequency modes associated with the pendulum-like motion of the helicopter body in pitch and roll around shaft axis. These frequencies for our Xcell-60 with the avionics payload are 2.7 and 3.1 Hz in pitch and roll, respectively, as was clearly seen in power spectral densities of the pitch and roll rate signals. The slightly higher roll frequency is due to lower roll inertia. These inputs have amplitudes of up to 6 deg/sec, and are attenuated with digital notch filters. The phase lag introduced by the filters is small enough to allow 70 degree phase margin in PI rate tracking loops, taking into account servo lags.

Lastly, the high hobby gyro gain leads to increased vibration levels. There are two main reasons for this phenomenon: the airframe flexibility couples into gyro measurement leading to resonances; and the flexible tail rotor servo pushrod, which acts like a second order system, and decreases the phase margin in the yaw rate control loop. We have stiffened the flexible nose of the airframe and installed a stiff pushrod to allow use of a higher yaw gyro gain. These modifications lead to better handling in manual flight.

FUTURE WORK

The next step on the way to fully autonomous aggressive maneuvers is to create a wide-envelope helicopter model, adequate for control law design. We have developed a non-linear 6 DOF helicopter model and tuned its response to flight data in hover. Work on modeling forward flight dynamics is in progress. As an intermediate step to demonstrating autonomous aggressive maneuvers, we are planning to implement a body axis velocity/heading rate-tracking controller.

ACKNOWLEDGEMENTS

David Vos has made invaluable contributions to the design of the avionics system. His insight was also essential to the elimination of vibration problems. Our thanks to the test pilot, Raja W. Bortcosh. David Dugail helped with analysis of governor response and preparation of this paper. Emilio Frazzoli facilitated development of the simulation framework. Financial support for this program was provided by AFOSR under grant F49620-99-1-0320, the Charles Stark Draper Laboratory, under IR&D grant DL-H-505334 and the Office of Naval Research, under Young Investigator Award N-00014-99-1-0668.

REFERENCES

[1] Padfield, G.D., 1996,
Helicopter flight dynamics: the theory and application of flying qualities and simulation modeling,
AIAA Education Series, Washington, DC.

[2] Mettler, B., Tischler, M. and Kanade, T., May 1999,
System identification of small-size unmanned helicopter dynamics,
presented at the AHS 55th Forum, Montreal, Quebec, Canada.

[3] Bramwell, A.R.S., 1976,
Helicopter dynamics,
Wiley & Sons, NY.

[4] Harris, Cyril M., editor, 1995,
Shock and vibration handbook,
McGraw-Hill, NY.

[5] Piedmonte, M. and Feron E., 1999,
Aggressive maneuvering of autonomous helicopters: a human-centered approach,
Proc. of 9th International Symposium on Robotics Research, pp. 413-419, Springer, US.

[6] R. Miller, O. Amidi, C. Thorpe and T. Kanade, 1999,
Precision 3-D modeling for autonomous helicopter flight,
Proc. of 9th International Symposium on Robotics Research, pp. 147-152, Springer, US. ■